Supporting Information for

Two-Dimensional Assembled PVP-Modified Silver Nanoprisms Guided by Butanol for Surface-Enhanced Raman Scattering-Based Invisible Printing Platforms

Kosuke Sugawa,*[a] Yutaro Hayakawa,[a] Yukiko Aida,[b] Yuto Kajino,[b] Kaoru Tamada*[b]

[a]*Department of Materials and Applied Chemistry, College of Science and Technology, Nihon University, Kanda-Surugadai, Chiyoda-ku, Tokyo 101-8308, Japan*

[b]*Institute for Materials Chemistry and Engineering (IMCE), Kyushu University, 744 Motooka, Nishiku, Fukuoka 819-0395, Japan*

1. Experimental section.

1-1. Materials.

Milli-Q water (resistivity: 18.2 MΩ cm) was used to prepare all aqueous solutions. Sodium tetrahydroborate ($NaBH_4$, Fujifilm Wako Pure Chemical (Japan)), silver nitrate ($AgNO_3$, Fujifilm Wako Pure Chemical (Japan)), PEI (MW: ~ 10,000, Fujifilm Wako Pure Chemical (Japan)), PVP (MW: ~55,000, Sigma–Aldrich (United States)), trisodium citrate dihydrate (Kanto Chemical (Japan)), sodium hydroxide (NaOH, Kanto Chemical (Japan)), MHA (Sigma–Aldrich (United States)), BuOH (Kishida Chemical (Japan)), EtOH (Kishida Chemical (Japan)), MeOH (Kishida Chemical (Japan)), acetone (Kishida Chemical (Japan)), EG (Kanto Chemical (Japan)), chloroauric(III) acid tetrahydrate (Nacalai Tesque (Japan)), and L-ascorbic acid (Tokyo Chemical Industry (Japan)) were used without further purification.

1-2. Synthesis of AgPRs.

AgPRs were synthesized by a previously described photochemical method.[S1] A freshly prepared aqueous solution including $NaBH_4$ (0.2 mM, 1 mL) as a reductive agent and trisodium citrate (5 mM, 100 mL) as a stabilizer was added to an aqueous solution including $AgNO_3$ (1 mL, 100 mL) in an ice bath, and the mixture was then stirred for 1 h to form silver nanospheres with an average diameter of 10 nm. After the pH of the silver colloidal aqueous solution was controlled to 11.2 by the addition of an aqueous solution of NaOH (0.2 M), the solution (10 mL in a 50-mL sample vial) was irradiated for 24 h with light from homebuilt 3 × 3 light-emitting diode (LED) arrays (OptoSupply, 5,800 mcd, 50% power angle: 60 deg) prepared on printed wiring boards with a centre wavelength of 470 ± 5 nm, which resulted in the formation of AgPRs.

The method for the synthesis of AgPRs employed in this study was based on photochemical shape transformation, which is intrinsically different from thermal synthesis.[S2,S3] Photochemical synthesis is advantageous for controlling the edge length of Ag nanoprisms compared with thermal synthesis. For example, in this study, both Ag nanoprisms with larger and shorter edge lengths were synthesized by simply controlling the wavelength of irradiation light (see 1-4). In addition, the plasmon bands of photochemically synthesized Ag nanoprisms tended to be sharper than those of thermally synthesized Ag nanoprisms.

1-3. Surface modification of AgPRs.

An EtOH solution of MHA (5 mM, 900 μL) was added to a colloidal aqueous solution of AgPRs (15 mL) protected with citric acid, and the mixture was stirred for 15 min to form self-assembled monolayers (SAMs) of MHA on the Ag surface. The resulting mixed solution was purified by centrifugation (15,000 rpm, 30 min), and the precipitate was dispersed in 5 mL of EtOH. The purified colloidal EtOH was rapidly added to an EtOH solution of PEI (4 mg/mL, 15 mL), and the mixture was stirred for 15 min, which resulted in the modification of PEI on the MHA SAM-modified AgPRs through the electrostatic interaction between the carboxyl groups and positively

charged PEI. The mixed solution was purified by centrifugation (15,000 rpm, 30 min), and the precipitate was dispersed in 5 mL of EtOH. The purified colloidal EtOH was added to an EtOH solution of PVP (0.7 mM, 15 mL), and the mixture was stirred for 15 min. The mixed solution was purified by two centrifugation steps (15,000 rpm, 30 min) using BuOH (1 mL) as a dispersion solvent.

1-4. Synthesis of gold nanospheres, large AgPRs, and gold nanostars.

Gold nanospheres were synthesized using a modified version of the Turkevich method.[S4] After refluxing an aqueous solution (100 mL) of 0.01 wt.% chloroauric(III) acid tetrahydrate for 30 min, an aqueous solution (4 mL) of 1 wt.% trisodium citrate dihydrate was added to the refluxing solution. Refluxing was then continued for another 1 h, which resulted in the formation of gold nanospheres with a diameter of 16 ± 2 nm.

Larger AgPRs were synthesized according to our previous report.[S1] First, silver nanospheres with an average diameter of 10 nm were synthesized in the same manner as AgPRs. Subsequently, the colloidal aqueous solution in which the pH was adjusted to 11.2 was irradiated with LED arrays with centre wavelengths of 470 nm for 2 h and 550 nm for 30 h, which resulted in the formation of larger AgPRs.

Gold nanostars were synthesized by adding an aqueous solution of ascorbic acid to a mixed solution consisting of water (100 mL), a colloidal solution of citric acid-modified gold nanospheres (1 mL), an aqueous solution of 2 mM $AgNO_3$ (1 mL), and an aqueous solution of 1 M NaOH (700 μL) under stirring.[S5]

These synthesis conditions were optimized to obtain uniformly sized nanoparticles for self-assembly.

1-5. Measurements.

Extinction spectra were recorded with a JASCO V-770 spectrophotometer. TEM observation was conducted using a Hitachi HF-2000 with an acceleration voltage of 200 kV. SERS spectra were measured using a micro-Raman spectrometer (NRS-4100). The excitation source was a CW laser with an excitation wavelength of 532 nm and a power of 0.4 mW adjusted through a neutral density filter. The laser was focused onto the sample surface using an objective lens (20× magnification). SERS mapping measurements were obtained by X-Y two-dimensional multipoint Raman measurement (exposure time: 10 s, integration count: 1) with a grid spacing of 150 μm. The surface tension of a mixed water/BuOH (EtOH and acetone) (= 20/1 volume ratio) solvent was measured using the Wilhelmy plate method with a standard platinum plate as the probe at room temperature (20 °C).

2. Zeta potentials of surface-modified AgPRs.

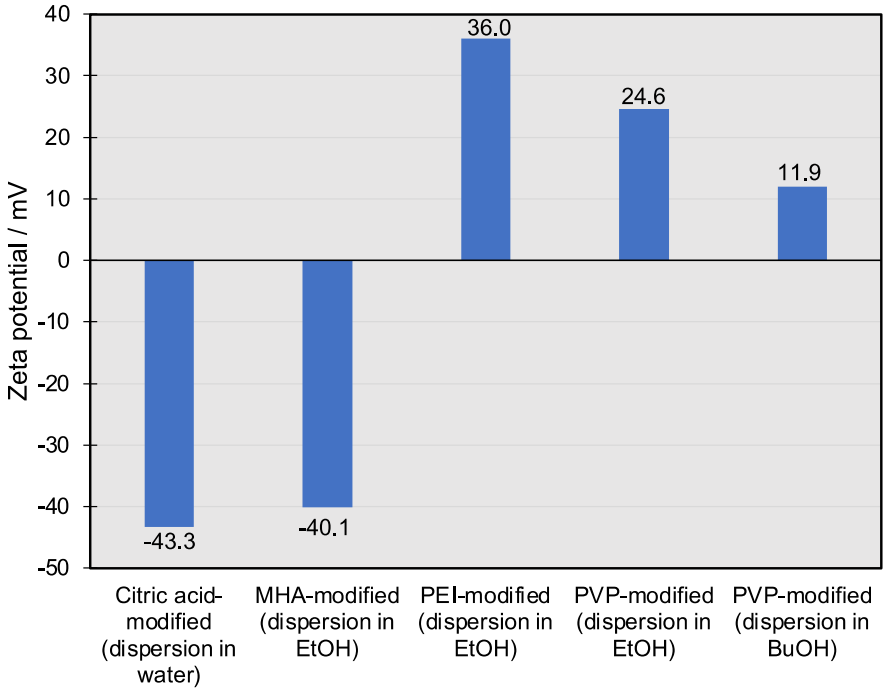

Figure S1. Change in the zeta potentials of AgPRs induced by modification with MHA, PEI, and PVP.

The surface modifications of AgPRs were tracked by measuring the change in the zeta potential of AgPRs (**Figure S1**). Citric acid-protected AgPRs showed a high negative potential (-43.3 mV) in water because of the abundance of carboxyl groups on their surface. After modification with MHA monolayers, the high negative potential was maintained in EtOH due to the presence of the terminal carboxyl group of MHA (-40.1 mV). In contrast, the potential of AgPRs in EtOH after modification with PEI largely shifted to a positive potential (36.0 mV), which is due to the abundance of amino groups contained in PEI. Furthermore, the potential of the AgPRs decreased by 11.4 mV in EtOH upon modification with PVP because PVP is a nonionic polymer. AgPRs were dispersed in BuOH during the self-assembly process at the air/water interface. The zeta potential of AgPRs in BuOH was even lower (11.9 mV) than that in EtOH because the polarity of BuOH is lower than that of EtOH.

3. Self-assembly at higher temperatures.

Figure S2. Photograph of the air-water interface 50 min after the addition of colloidal BuOH of AgPRs into water at 45 °C in a petri dish. Approximately 80% of the water surface was covered with AgPR assemblies in 50 min, but the AgPR assemblies became nonuniform.

4. SEM images of an AgPR film on a Si wafer.

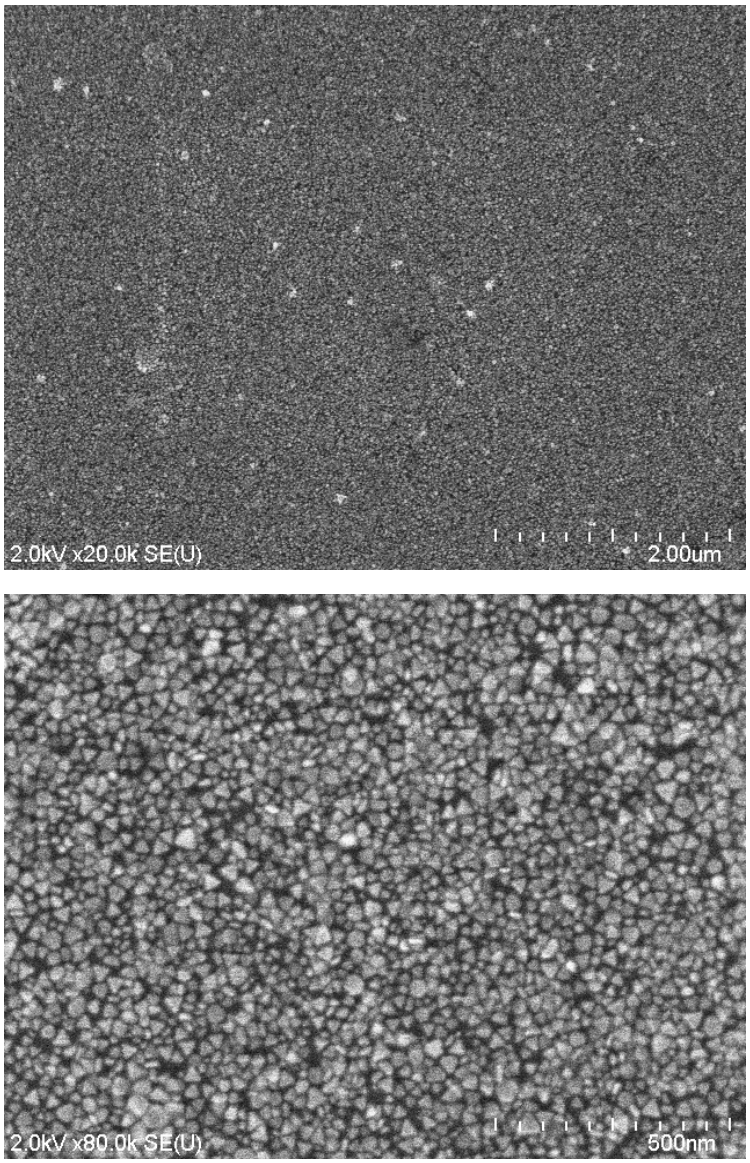

Figure S3. SEM images of an AgPR film transferred onto a Si wafer.

5. Optical properties of a mixed colloidal solution of AgPRs during the self-assembly process.

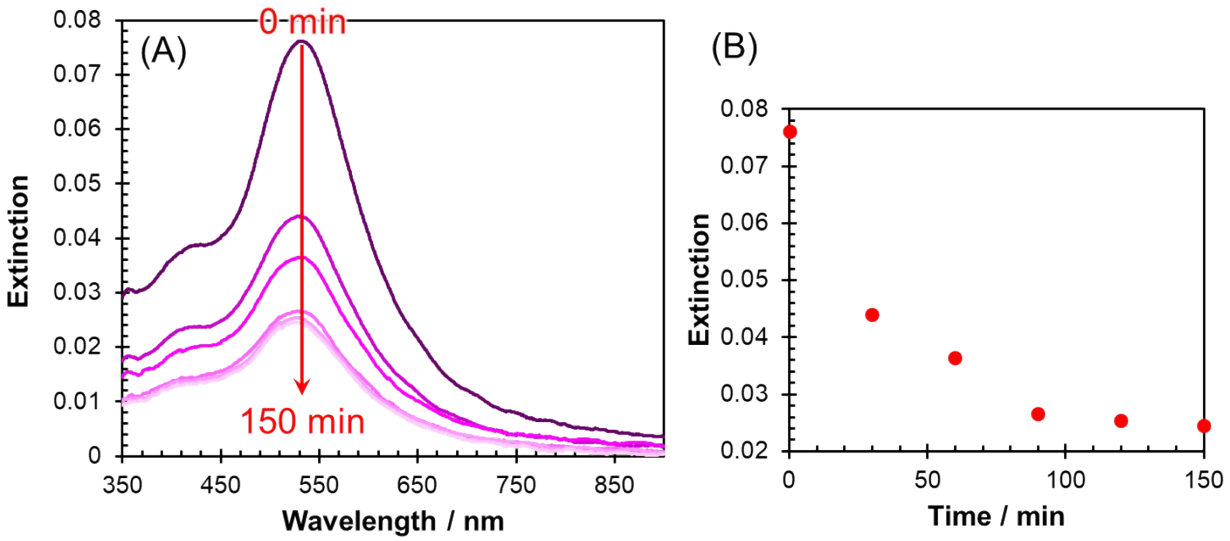

Figure S4. Extinction spectra of a mixed colloidal solution after the addition of a colloidal butanol solution of AgPRs to Milli-Q water in a petri dish. Time course of the (A) extinction spectra and (B) maximum extinction intensity of the aqueous dispersion solution (20-fold dilution) after addition of the colloidal butanol solution of AgPRs to water in a petri dish.

6. Influence of mixing solvents (MeOH and ethylene glycol) on AgPR assembly.

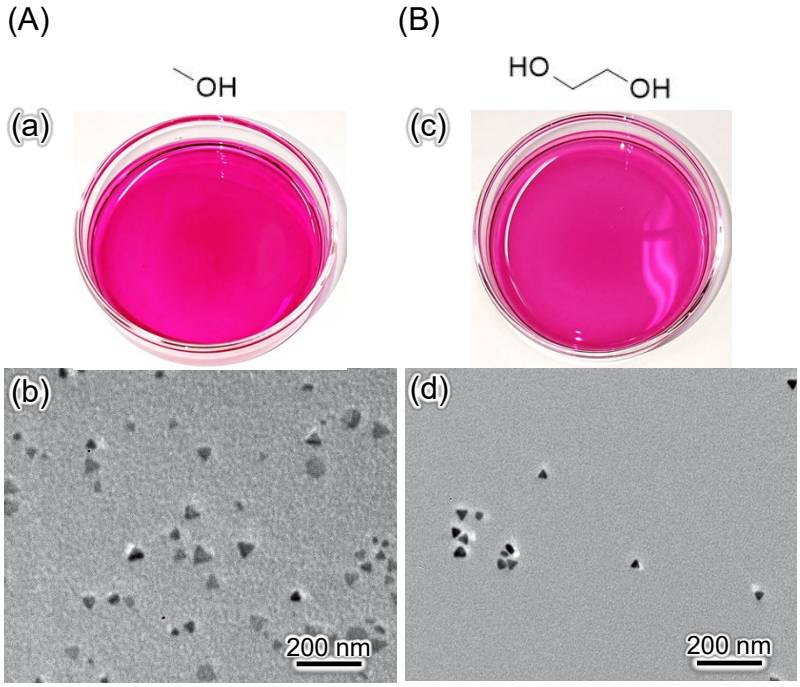

Figure S5. Influence of mixing solvents on AgPR assembly: (A) MeOH and (B) ethylene glycol. Photographs ((a) and (c)) of the air-water interface after 2 h and TEM images of the transferred films ((b) and (d)) when MeOH and ethylene glycol were used as the mixing solvents, respectively.

7. Self-assembly of AgPRs in closed and opened systems.

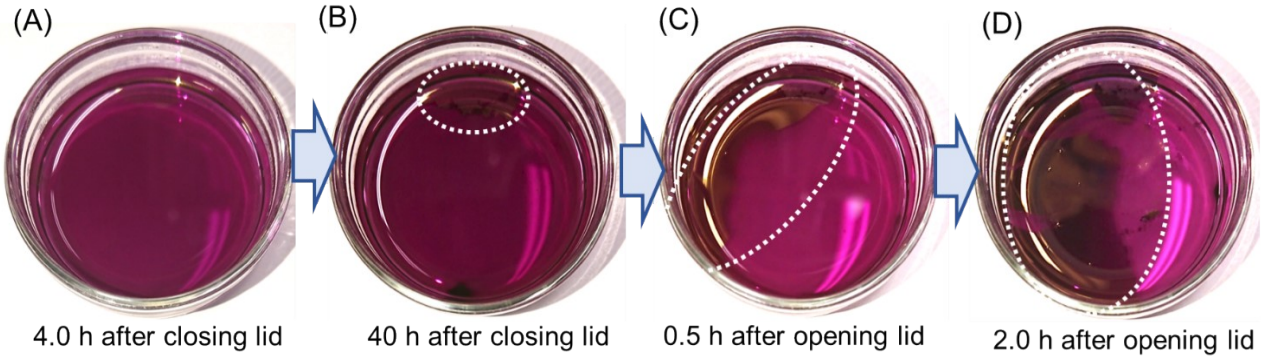

Figure S6. Verification that an open system is necessary for the assembly AgPRs. Photographs obtained (A) 4 h after closing the lid immediately after adding a colloidal BuOH (400 μL) solution of AgPRs to Milli-Q water (8000 μL), (B) 40 h after closing the lid, (C) 0.5 h after opening the lid, and (D) 2.0 h after opening the lid.

When a colloidal BuOH solution of AgPRs was added to Milli-Q water and the mixed colloidal solution in a petri dish was then covered with a lid, no AgPR assemblies were formed even after 40 h. Subsequently, when the lid was opened, AgPR assemblies soon began to form at the air/water interface.

8. Extinction spectra of a colloidal aqueous solution and a colloidal BuOH/water (= 1/20 vol.%) solution of MHA-PEI-PVP-modified AgPRs.

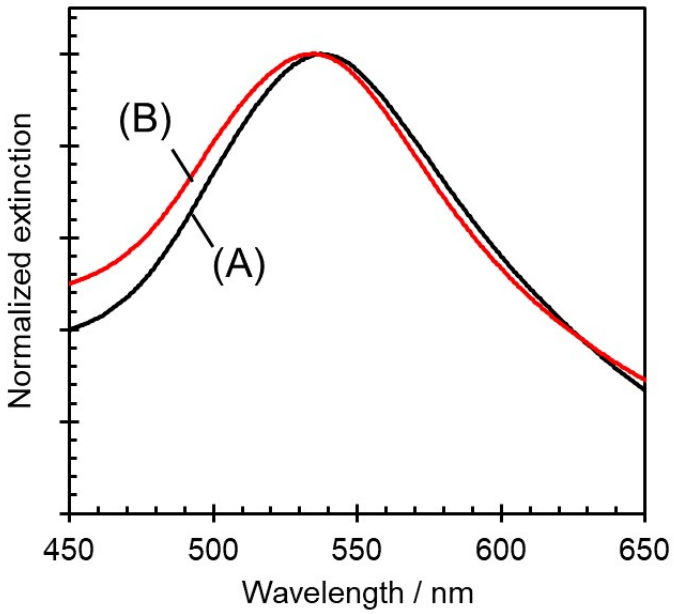

Figure S7. Extinction spectra of (a) a colloidal aqueous solution and (b) a colloidal water/BuOH (= 20/1 volume ratio) solution of MHA-PEI-PVP-modified AgPRs.

After the PVP modification process, which is described in the Experimental Section, the colloidal EtOH solution of AgPRs was centrifuged (15,000 rpm, 30 min), and the precipitate was then dispersed in Milli-Q water. Similarly, the MHA-PEI-PVP-modified AgPRs were also dispersed in a mixed solvent of Milli-Q water/BuOH (= 20/1 volume ratio). The extinction spectra of both colloidal solutions are shown in Figure S5. As mentioned in the manuscript, the LSP resonance wavelength of AgPRs responds sensitively to a change in the local refractive index around them. Assuming that water and BuOH are uniformly mixed in the mixed solvent, if the change in the LSP resonance wavelength is due to the difference in the refractive index of the dispersed solvent, the LSP resonance wavelength of AgPRs dispersed in the mixed solvent should be generated at a slightly longer wavelength than that of AgPRs dispersed in water because the refractive index of the mixed solvent (n = 1.3365, calculated using the Lorentz–Lorenz equation[S6]) is slightly higher than that of water (n = 1.3334). However, the extinction peak of AgPRs dispersed in the mixed solvent was generated at a shorter wavelength by 3 nm than that of AgPRs dispersed in water. The change in resonance wavelength can be explained by the swelling of PVP with BuOH. [S7] The LSP resonance wavelength should be shifted to a shorter wavelength with a reduction in the density of the surrounding PVP with a high refractive index (n = 1.53-1.57) in the outermost layer of AgPRs due to the swelling associated with the adsorption of BuOH.

9. Zeta potential of PVP-modified AgPRs dispersed in water and water/BuOH (= 20/1 volume ratio).

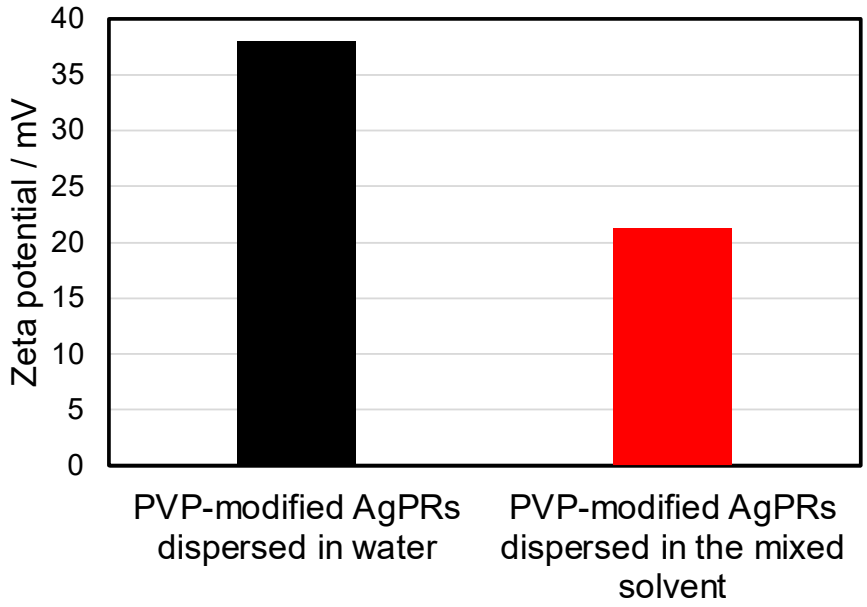

Figure S8. Zeta potential of PVP-modified AgPRs dispersed in water and water/BuOH (= 20/1 volume ratio).

PVP-modified AgPRs were dispersed in Milli-Q water and a mixed Milli-Q water/BuOH (= 20/1 volume ratio) solvent in a similar manner as described in the legend of Figure S4. As shown in Figure S6, the zeta potential of PVP-modified AgPRs (21.3 mV) dispersed in the mixed solvent was significantly lower than that (37.9 mV) in Milli-Q water.

10. Change in the surface tension of the mixed solvent consisting of water/BuOH (= 20/1 volume ratio).

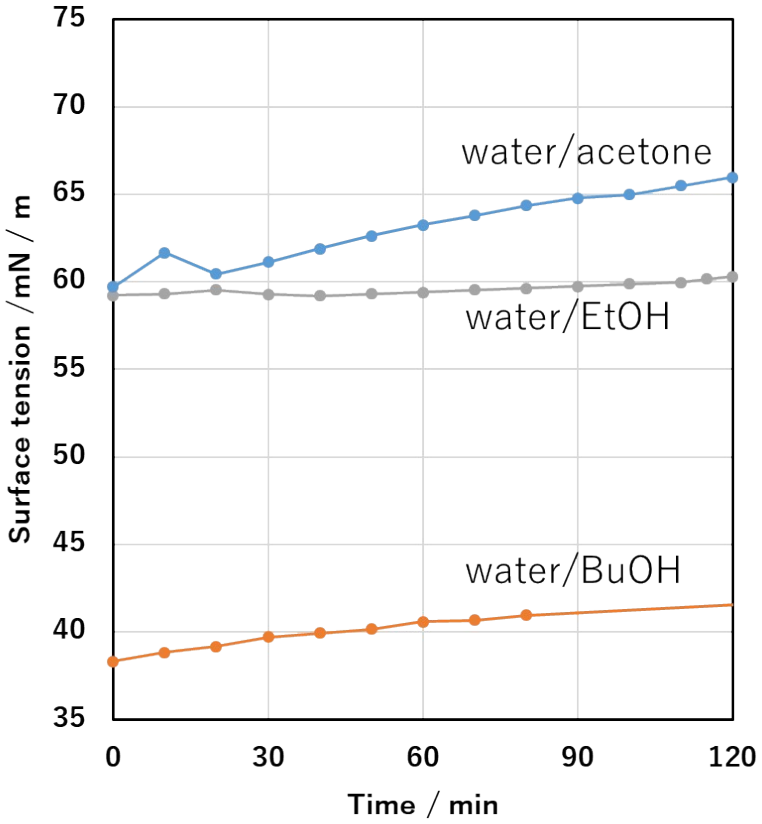

Figure S9. Plots of the surface tension of the mixed solvents consisting of water/BuOH, water/EtOH and water/acetone (= 20/1 volume ratio) over time in an open system. All the measurements were conducted at 19.0±1 °C with a Pt plate.

The time course of the surface tension of the mixed water/BuOH solvent is shown in Figure S7. Immediately after the start of the measurement, the surface tension was significantly lower than that of water (72.53 mN m^{-1} at 20 °C). This result shows the adsorption of BuOH on the air/water interface due to the strong surface activity of BuOH. In addition, the surface tension gradually increased over time because BuOH preferentially volatilized over water from the mixed solvent, and the molar concentration of BuOH decreased. Moreover, the surface tensions of water/EtOH and water/acetone were similar and significantly higher than that of the water/BuOH system.

11. SERS assignments of 4-MBA adsorbed on AgPR assemblies.[S8,S9]

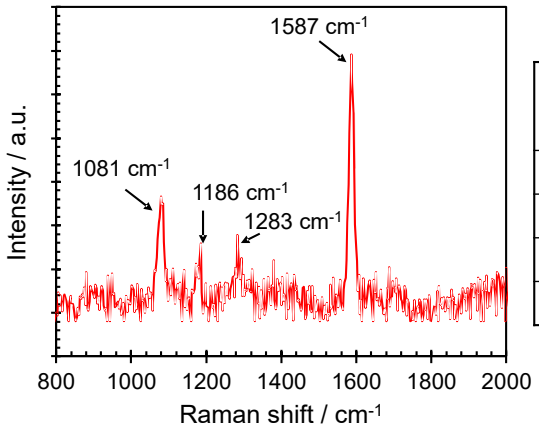

Wavenumber (cm^{-1})	Band assignments
1081	In-plane ring breathing + *n* (C–S)
1186	*n* (CH)
1283	*n* (C−OH)
1587	Totally symmetric *n* (CC)

ν = stretching

Figure S10. SERS assignments of 4-MBA on AgPR assemblies.

References

S1. N. Takeshima, K. Sugawa, M. Noguchi, H. Tahara, S. Jin, K. Takase, J. Otsuki, K. Tamada, *Chem. Lett.*, 2020, 49, 240-243.

S2. I. Pastoriza-Santos, L. M. Liz-Marzan, *Nano. Lett.* 2002, **2**, 903-905.

S3. Y. Yang, S, Matsubara, L. Xiong, T. Hayakawa, M. Nogami, *J. Phys. Chem. C* 2007, **111**, 9095-9104.

S4. J. Turkevich, P. C. Stevenson, J. Hillier, *Discuss. Faraday Soc.*, 1951, **11**, 55-75.

S5. I. G. Theodorou, P. Ruenraroengsak, D. A. Gonzalez-Carter, Q. Jiang, E. Yague, E. O. Aboagye, R. C. Coombes, A. E. Porter, M. P. Ryan, F. Xie, *Nanoscale*, 2019, **11**, 2079-2088.

S6. H. Chen, X. Kou, Z. Yang, W. Ni, J. Wang, *Langmuir*, 2008, **24**, 5233-5237.

S7. G. K. Joshi, K. A. Smith, M. A. Johnson, R. Sardar, *J. Phys. Chem. C*, 2013, **117**, 26228-26237.

S8. W. K. H. Ho, Z. Y. Bao, X. Gan, K.-Y. Wong, J. Dai, D. Lei, *J. Phys. Chem. Lett.*, 2019, **10**, 4692-4698.

S9. Y. Wang, W. Ji, H. Sui, Y. Kitahama, W. Ruan, Y. Ozaki, B. Zhao, *J. Phys. Chem. C*, 2014, **118**, 10191-10197.